# High-Fidelity Multi-Rotor Unmanned Aircraft System Simulation Development for Trajectory Prediction Under Off-Nominal Flight Dynamics

John V. Foster [1]
*NASA Langley Research Center, Hampton, VA, 23681-2199*

David C. Hartman[2]
*Drexel University, Philadelphia, PA, 19104*

**The NASA Unmanned Aircraft System (UAS) Traffic Management (UTM) project is conducting research to enable civilian low-altitude airspace and UAS operations. A goal of this project is to develop probabilistic methods to quantify risk during failures and off-nominal flight conditions. An important part of this effort is the reliable prediction of feasible trajectories during off-nominal events such as control failure, atmospheric upsets, or navigation anomalies that can cause large deviations from the intended flight path or extreme vehicle upsets beyond the normal flight envelope. Few examples of high-fidelity modeling and prediction of off-nominal behavior for small UAS (sUAS) vehicles exist, and modeling requirements for accurately predicting flight dynamics for out-of-envelope or failure conditions are essentially undefined. In addition, the broad range of sUAS aircraft configurations already being fielded presents a significant modeling challenge, as these vehicles are often very different from one another and are likely to possess dramatically different flight dynamics and resultant trajectories and may require different modeling approaches to capture off-nominal behavior. NASA has undertaken an extensive research effort to define sUAS flight dynamics modeling requirements and develop preliminary high-fidelity six degree-of-freedom (6-DOF) simulations capable of more closely predicting off-nominal flight dynamics and trajectories. This research has included a literature review of existing sUAS modeling and simulation work as well as development of experimental testing methods to measure and model key components of propulsion, airframe and control characteristics. The ultimate objective of these efforts is to develop tools to support UTM risk analyses and for the real-time prediction of off-nominal trajectories for use in the UTM Risk Assessment Framework (URAF). This paper focuses on modeling and simulation efforts for a generic quad-rotor configuration typical of many commercial vehicles in use today. An overview of relevant off-nominal multi-rotor behaviors will be presented to define modeling goals and to identify the prediction capability lacking in simplified models of multi-rotor performance. A description of recent NASA wind tunnel testing of multi-rotor propulsion and airframe components will be presented illustrating important experimental and data acquisition methods, and a description of preliminary propulsion and airframe models will be presented. Lastly, examples of predicted off-nominal flight dynamics and trajectories from the simulation will be presented.**

## Nomenclature

| | | |
|---|---|---|
| A | = | rotor reference area |
| $A_{VRS}$ | = | amplitude of vortex ring state thrust variation |
| $C_l$ | = | aerodynamic rolling moment coefficient |
| $C_m$ | = | aerodynamic pitching moment coefficient |
| $C_N$ | = | aerodynamic normal force coefficient |

[1] Senior Research Engineer, Bldg 1232/Mail Stop 308, john.v.foster@nasa.gov, AIAA Associate Fellow.
[2] Ph.D. Candidate, Department of Mechanical Engineering, dh578@drexel.edu, AIAA Member

$C_Q$ = rotor torque coefficient
$C_T$ = rotor coefficient of thrust
$C_x$ = force coefficient in the *x* direction
$C_y$ = force coefficient in the *y* direction
COTS = commercial off the shelf
D = propeller diameter, ft
DOF = degrees of freedom
ESC = electronic speed control
J = propeller advance ratio
LPF = low-pass filter
LQR = Linear Quadratic Regulator control architecture
$m_i$ = denotes i-th motor
$mw_i$ = denotes motor-wind axis for i-th motor
NASA = National Aeronautics and Space Administration
Q = rotor axial torque
$\bar{q}$ = dynamic pressure, psf
RPM = revolutions per minute
RPS = revolutions per second
sUAS = small UAS
T = rotor thrust
UAS = unmanned aircraft system
URAF = UTM Risk Assessment Framework
UTM = UAS Traffic Management
V = total airspeed, ft/s
$i$ = rotor incidence angle, positive for wind from above disk, as in forward flight.
$\alpha$ = angle of attack, deg
$\beta$ = angle of sideslip, deg
$\mu_x$ = rotor advance ratio
$\mu_z$ = normal velocity ratio
$\nu_h$ = induced velocity during hover
$\omega_{VRS}$ = VRS frequency
$\Omega$ = rotor speed, radians per second
$\rho$ = air density, lb-sec$^2$/ft$^4$

## I. Introduction

THE NASA Unmanned Aircraft System (UAS) Traffic Management (UTM) project is leading the development and demonstration of a possible future system that could safely enable low-altitude airspace and UAS operations.

As part of this project, research and development of probabilistic methods to quantify risk during failures and off-nominal flight conditions is currently in progress.[1–4] An important requirement for a risk assessment system is the prediction of feasible trajectories during off-nominal events such as control failure, atmospheric upsets, or navigation anomalies that can cause large deviations from the intended flight path or extreme vehicle upsets beyond the normal flight envelope. Few examples of high-fidelity modeling and prediction of off-nominal behavior for small UAS (sUAS) vehicles exist, and modeling requirements for accurately predicting flight dynamics for out-of-envelope or failure conditions are essentially undefined. In addition, the broad range of sUAS aircraft configurations already being fielded presents a significant modeling challenge, as these vehicles are often very different from one another and are likely to possess dramatically different flight dynamics and resultant trajectories and may require different modeling approaches to capture off-nominal behavior.

NASA has undertaken a research effort to define sUAS flight dynamics modeling requirements and develop preliminary high-fidelity six degree-of-freedom (6-DOF) simulations capable of more closely predicting off-nominal flight dynamics and trajectories. This research has included a literature search of existing sUAS modeling and simulation work as well as development of experimental test methods to measure and model key components of propulsion, airframe and control characteristics. The primary objective of these efforts is to develop tools to support UTM risk analyses[1,2] and for the real-time prediction of off-nominal trajectories for use in the UTM Risk Assessment Framework (URAF).[3] Additionally, this deeper knowledge of sUAS flight dynamics gained is expected to provide

opportunities for improved aircraft design and in developing robust control strategies able to better manage or avoid off-nominal flight conditions.

This paper provides an overview of recent NASA off-nominal modeling and simulation research for a generic quad-rotor configuration typical of many commercial vehicles in use today. An overview of relevant off-nominal multi-rotor behaviors will be presented in Section II to define modeling goals and to identify the prediction capability lacking in simplified models of multi-rotor performance. Section III presents a limited literature review for assessing the current state-of-the-art and availability of relevant modeling data. In section IV, a description of recent NASA wind tunnel testing of multi-rotor propulsion and airframe components will be presented illustrating important experimental and data acquisition methods, and a description of preliminary propulsion and airframe models will be presented. Lastly, examples of predicted off-nominal flight dynamics and trajectories from a six-degree-of-freedom simulation using the wind tunnel data will be presented in Section V.

## II. Approach and Objectives

Off-nominal modeling and simulation of aircraft has been the subject of research for decades and has often been motivated by the need to understand aircraft flight characteristics leading to loss of control events. High-angle-of-attack maneuvering and departure prevention for fighter aircraft motivated extensive research on modeling complex separated flows that led to many advances in the prediction of complex motions such as departure from controlled flight and spins[5]. In recent years, simulation of large transport aircraft received attention to improve stall and post-stall modeling for pilot training simulators[6]. With the rapid introduction of small Unmanned Aircraft Systems (sUAS) vehicles, a new challenge has emerged in predicting loss-of-control susceptibility and off-nominal trajectories for unconventional configurations, many with no lifting surfaces. This is leading to new research designed to address aerodynamic and propulsion modeling methods as well as experimental methods for characterizing flight dynamics. Specifically, multi-rotor configurations present unique modeling challenges due to the potential for massively separated flows, propulsion-dominated dynamics, and complex flow interactions between the rotors and airframe.

The current research is being conducted under the Safety and Risk Assessment element of the NASA UTM program. The primary goal is to develop modeling and simulation methods for sUAS vehicles that can be used for risk assessment and potentially as part of an integrated autonomous traffic management system. Due to the wide range of potential sUAS configurations, emphasis is placed on addressing the feasibility of generic trajectory modeling rather than type-specific models. In addition, the need for predictive tools and simulations that can be implemented in rapid or near real-time algorithms is being considered.

The research described in this paper is focused on multi-rotor configurations, which present complex modeling challenges but for which relatively little modeling data has been published, particularly for off-nominal or out-of-envelope flight conditions. An experimental approach for the development of the aerodynamic and propulsion database is being used for this effort. Existing wind tunnel test methods, previously developed to characterize flight dynamics under large flow angles and dynamic motions are being leveraged and advanced for this research. A six degree-of-freedom simulation has been developed to support studies of out-of-envelope flight dynamics and the associated non-linear modeling requirements.

## III. Literature Review

The complexities of rotorcraft flight dynamics, such as for manned helicopters and tiltrotors, have been the subject of extensive study and are well documented. Decades of research, engineering effort, and experience have made manned rotorcraft increasingly safe and reliable, and resulted in robust methods for establishing operating restrictions to avoid development of unsafe flight conditions. Examples include limitations on maximum forward speed, often dictated in part by retreating blade stall or tip Mach number; limitations on descent rate and approach profile, determined to avoid vortex ring state (VRS) and settling with power; and other flight-envelope and maneuvering restrictions intended to avoid overstressing the aircraft structure or powerplant[7]. For developing models of off-nominal performance for sUAS multirotors, it is reasonable to suspect that many of these same phenomena can be considered, while also acknowledging that differences in scale may significantly affect off-nominal behaviors. However, despite the popularity of the platform, not much attention has been focused on investigating these limitations or developing methods for modeling performance outside of nominal flight conditions.

A number of different approaches to multirotor sUAS modeling have been introduced in the literature, often taking a form conducive to control development or to meet a specific purpose unique to the author's focus. For example, an overview of a typical modeling approach which includes the sometimes neglected influence of blade-flapping, is shown in Ref [8]. Models have also been developed to address issues of inaccurate state-estimation from sensor data; an example is presented in Ref. [9]. Specific model extensions have also appeared to support study of unusual flight conditions or unique aircraft designs. Examples include an experiment-supported investigation of relaxed-hover

equilibrium stabilization,[10] which requires consideration of body-rotation-induced drag; and modeling efforts specific to multirotor sUAS with tilted motor axes.[11] Other models of varying complexity have been used to compute feasible flight trajectories meeting specified criteria, see e.g. Refs. [12, 13]. Many of the published models have been used for model-based feedback-control design, often with demonstrated success. It has been well documented that in many of the flight conditions commonly considered, various forms of appropriately designed feedback control can overcome model inaccuracies and provide satisfactory flight performance.

Most of the models appearing in the available literature do not account for variations in rotor performance with the velocity and incidence angle of airflow relative to the rotor disk. Therefore, while appropriate for modeling flight near hover, they may be unsuitable under off-nominal flight conditions in which these aspects of rotor performance become increasingly influential on aircraft behavior. Ref. [14] uses basic methods from helicopter theory to predict changes in performance due to inflow angle and velocity, as well as noting from experiment the presence of apparent interaction effects between the airframe and rotor-inflow and wake. The expected theoretical behavior of rotor inflow velocity is modeled for a range of flight conditions, and some experimental work is described for modeling of blade-flapping-induced moments and drag force.

Published experimental investigations of rotor performance are mostly concerned with full-scale rotors for manned aircraft. The wind-tunnel test methods used vary significantly between authors and applications. Off-nominal performance related to VRS is specifically targeted in Ref. [15] and [16], which study performance characteristics of an experimental model representative of a tiltrotor under descending flight and VRS conditions. In Ref. [17], Johnson provides a broad survey of VRS related flight tests and wind tunnel experiments, and develops an empirical model for induced velocity that matches momentum theory at the limits of the VRS region. Johnson finds that across all of the experimental investigations surveyed, VRS consistently presents as a reduction in mean thrust, unsteady thrust fluctuations about the mean, and a reduction in the lift curve slope. The unsteady fluctuations in thrust appear to occur with varying frequency and severity, and their relationship to other fundamental characteristics of the rotor are not specified. It is documented that tiltrotor aircraft such as the V-22 exhibit VRS primarily as “roll-off”, where the aircraft undergoes an un-commanded roll due to unequal and unsteady lift production from its rotors, and correct prediction of this behavior requires consideration for simulation development.[17] In multirotor sUAS, experimental results suggesting possible instability in descending flight have been reported.[18] Operators have described the development of un-commanded roll or pitch of the vehicle, usually resulting in unintended altitude loss. This condition can occur during either autonomous or human-piloted flight, and is sometimes colloquially referred to as the “wobble of death” by multirotor sUAS operators.

Besides experimental tests intended to study full-scale rotor systems, some wind tunnel testing has been reported on sUAS-scale propellers, including under off-nominal conditions. In Ref. [19], the authors explore propeller performance variation with Reynolds number, finding generally increased efficiency and thrust coefficient as Reynolds number increases. In Ref. [20], small propellers were tested with axial flow from directly beneath the rotor to determine the development conditions and performance effects of VRS at the sUAS propeller scale. Another experiment, reported in Ref. [18], documents performance under a large range of angles, and noted unsteadiness in descending flight (presumably due to VRS encounter or wake re-ingestion), and noted improved rotor-efficiency in slow forward flight versus a zero-airspeed hover. In Ref. [21], the authors tested not only isolated rotors, but several complete multirotor sUAS aircraft at a selection of test points representing a range of nominal flight conditions. These results have provided an important foundation for performance and trajectory modeling and the current research is aimed at building on these results.

## IV. Wind Tunnel Testing

### A. Approach

In support of the effort to model off-nominal flight dynamics, the present investigation has included wind tunnel testing across a wide envelope of conditions. This study also specifically targeted off-nominal flight conditions conducive to VRS and other unsteady and nonlinear aerodynamic behaviors, and time-history data were recorded to assess time-varying effects and quantify vibration forces and frequencies.

One issue explored is the potential for generic multi-rotor modeling via integration of isolated propulsion models for any number of rotors and rotor orientations. The interaction effects between rotors, as well as with the airframe, are important considerations being addressed by this research. Wind tunnel testing was conducted in three parts to assess individual contributions to total forces and moments, and these data were used for simulation modeling. Isolated propeller testing was conducted to acquire a 6-DOF model for propeller effects only, including thrust and torque. Subsequently the bare airframe alone was tested followed by the full powered vehicle.

**Figure 1. Front view of aircraft model in NASA LaRC 12-Foot wind tunnel.**

**Figure 2. Rear view of aircraft model in NASA LaRC 12-Foot wind tunnel.**

### B. Description of Test Vehicle

A commercial off-the-shelf (COTS) quadrotor was selected as the focus vehicle for wind tunnel testing which could ultimately be suitable for flight testing. This vehicle, shown in Fig.1 is the model XPX manufactured by XProHeli. The vehicle possesses an aluminum box airframe with four eMax MT4114, 340 kv motors mounted on 8.25 in. long arms. The propellers are 14 in. diameter multi-rotor propellers manufactured by Advanced Precision Composites, specifically the 14x5.5MR/MRP models. In addition, the arms are canted upward at an angle on this aircraft, resulting in the motors being tilted inward approximately 7 deg. The vehicle is designed to fly in the "X" configuration, with two arms pointed forward, or in the "+ (plus)" configuration with a single arm pointed forward. The airframe includes removable, rigid landing gear as well as an attachment plate for a camera on the underside of the aircraft. During wind tunnel testing, the airframe was sealed with tape to eliminate flow-thru effects and to be more representative of vehicles with enclosed airframes.

### C. Test Facility Description and Model Installation

The vehicle was tested in the NASA Langley 12-Foot Low-Speed Tunnel. This facility includes the capability for static and dynamic force and moment measurements and includes a rigid sting operated on a C-strut with a maximum pitch rotation of +90°. In addition, the sting can be rolled inverted which allows the capability to test to -90° relative to the air flow. The facility is capable of testing at dynamic pressures from 0.3 to 7 psf. The facility also has provisions for flow visualization as well as high-speed video.

The model was modified to allow rigid mounting in the wind tunnel by adding a stiffener plate to the bottom of the airframe to accommodate the mounting hardware. The vehicle was attached to a vertical post which was rigidly mounted to a straight sting and balance arrangement. Photos of the vehicle mounted in the tunnel are shown in Figs. 1and 2.

Force and moment measurements were acquired via a six-component strain gauge balance. The balance was selected to accommodate the anticipated loads while allowing high sample rates to be acquired. Balance accuracy for each axis varied from 0.03 to 0.11% based on the full load range. For the isolated propeller and airframe testing, the balance was covered by a sealed enclosure to eliminate wind effects on the balance. The data acquisition system recorded all balance measurements and sting angle as well as tunnel speed and temperature at data sample rates of 2500 Hz during isolated prop testing and 2,222 Hz during isolated-airframe and full-aircraft testing.

### D. Isolated Propeller Testing

*1. Test Apparatus and Methods*

A single propeller was tested to develop a six degree-of-freedom model of forces and moments under the range of flow angles and motor RPM. Static forces and moments were measured at fixed flow angles ranging from -90° to +90° relative to the motor shaft, typically expressed in terms of incidence angle ($i$) as shown in Fig. 3. Tunnel dynamic pressure and motor RPM were varied from 0.3 to 7 psf and

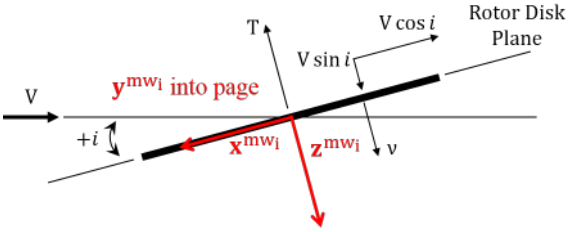


**Figure 3. Coordinates used for isolated propeller performance model. Positive incidence angle *i* occurs in forward flight as shown. Wind axes for each motor (labeled $mw_i$) are calculated independently to match relative wind conditions for each rotor.**

**Figure 4. Isolated propeller test configuration in NASA LaRC 12-Foot wind tunnel.**

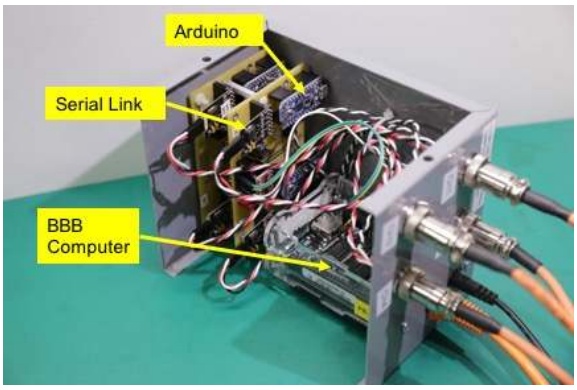


**Figure 5. Four-channel Serial Link ESC data acquisition and motor speed control system in enclosure.**

1,000 to 6,500 RPM respectively to acquire target values of advance ratio (J) ranging from 0 to 3. A photo of the isolated propeller test setup in shown in Fig. 4.

Because the capability to maintain a desired motor RPM under unknown loading conditions was critical for the purposes of this test, a closed-loop controller was developed to regulate the commanded motor RPM. This system utilized real-time RPM feedback from a Castle Creations Phoenix Edge 50 amp electronic speed controller (ESC) connected to a Castle Serial Link and an Arduino Teensy. The serial link was used to control the ESC throttle and gather real-time data, while the Arduino was used to measure commutation frequency of the motor. Both of these communicated with a control and data-collection program running on a Beagle Bone Black (BBB). The control program used proportional-integral feedback to regulate the motor RPM, and simultaneously recorded motor speed and other test parameters. A text-based interface was used to communicate with the BBB from a laptop and monitor parameters in real time. Time-history files for each test point were recorded at a sample rate of approximately 87 Hz for post-test analysis. An important limitation of this approach was that the motor controller was completely independent from the wind-tunnel data acquisition system, limiting the ability to cross-reference RPM time-histories with balance time-histories. An improved version of the motor control system is being developed that allows motor RPM data to be recorded by the wind-tunnel data collection system in real time. A photo of the motor speed control hardware is shown in Fig. 5.

The performance of this motor control system was satisfactory at all of the conditions tested, with no apparent steady-state error and a normalized standard deviation from commanded RPM of 1% or less. Motor RPM measurements showed increased scatter under experimental conditions when the rotor was operated in its own or another rotor's wake. Nevertheless, mean motor speeds remained stable even in these conditions. Under flight conditions in which the rotor was tilted into the wind and the advance ratio (J) was sufficiently high, the motor would begin to windmill and the motor controller would reach 0% throttle. Increasing the wind velocity or motor-tilt into the wind (positive incidence angle) would lead to further increase in windmilling RPM with an equilibrium rotation rate reached based on the wind speed, incidence angle, and the drag properties of the rotor and motor assembly. The present test condition database does not include a full characterization of windmilling; additional testing of power-off rotor behavior under various wind conditions is planned for future testing, as this behavior is expected to be influential on aircraft performance following complete motor failures.

*2. Method of Testing*

Test points were selected to cover a broad range of flight conditions, many of which are well outside of typical multirotor sUAS operating conditions. Conditions that were expected to generate VRS were targeted for additional coverage. Most test points were selected in terms of advance ratio (J), and combinations of motor speed and tunnel velocity were selected to match the desired value. Sweeps of incidence angle were performed while holding J constant. Wherever possible, given the motor and tunnel limitations, J values were tested at both high-RPM, low-wind velocity and low-RPM, high-wind velocity conditions. This procedure allowed assessment of the influence of rotor speed on performance.

For each test point, time-averaged data were recorded for the three force-axes and three moment-axes. In addition to this averaged value, 10 sec time histories were saved at a 2,500 Hz sample rate. The raw data were later post-processed for additional characterization of time-varying changes to performance.

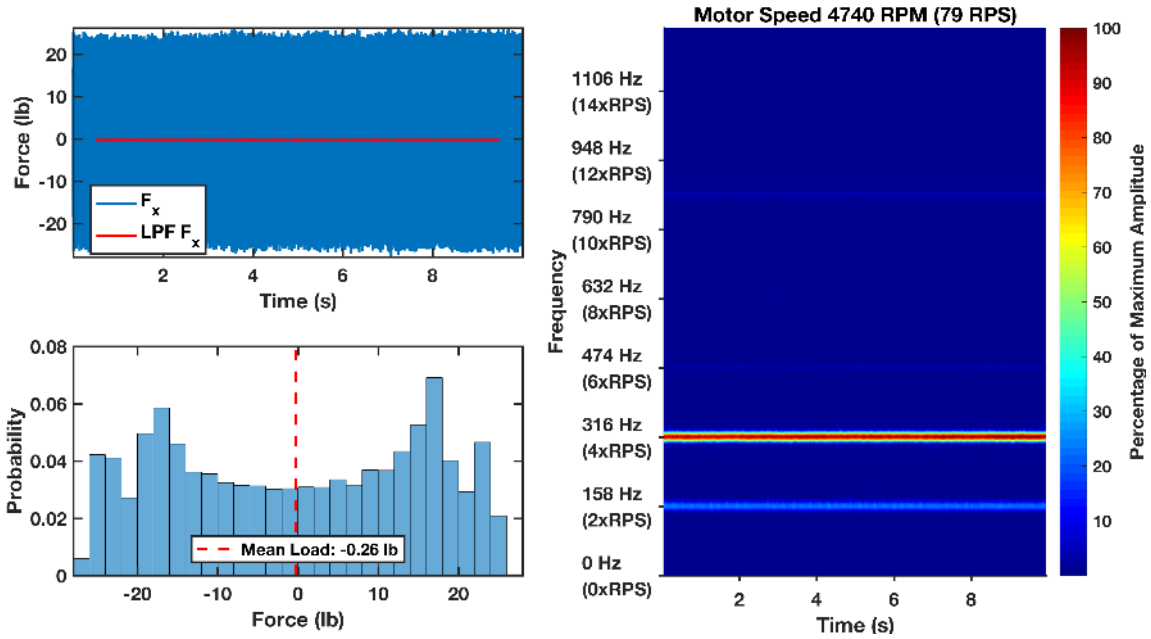


**Figure 6. Isolated rotor time-history and spectral analysis for force in the rotor x-axis. Incidence angle $i = 0°$, RPM $= 4,740$, V $= 66$ ft/s, J $= 0.72$.**

*3. Vibration Characterization*

Wind tunnel testing of the isolated propeller often yielded higher-magnitude periodic forces and moments than were anticipated prior to testing. Fig. 6 shows x-axis fore data for the isolated propeller at an incidence angle of 0° and at an advance ratio of J=0.72. Note that while the mean load is only about 0.25 lb. in the negative x-axis (i.e. in the direction of "drag" relative to the rotor disk), the peak periodic values reach almost ±25 lb. The spectrogram in the right plot shows a strong frequency component at a rate of four cycles per rotation and a weaker periodic force at two cycles per rotation. Similar vibration-inducing forces have been reported elsewhere[21]. Typically, periodic forces occurring at two cycles per rotation are associated with blade-flapping (for a two-bladed prop), while four cycle per rotation forces are sometimes attributed to vortex interaction, especially in multirotors where a rotor may operate within the wake of another rotor. Structural resonance is suspected to play a significant role in the severity of the

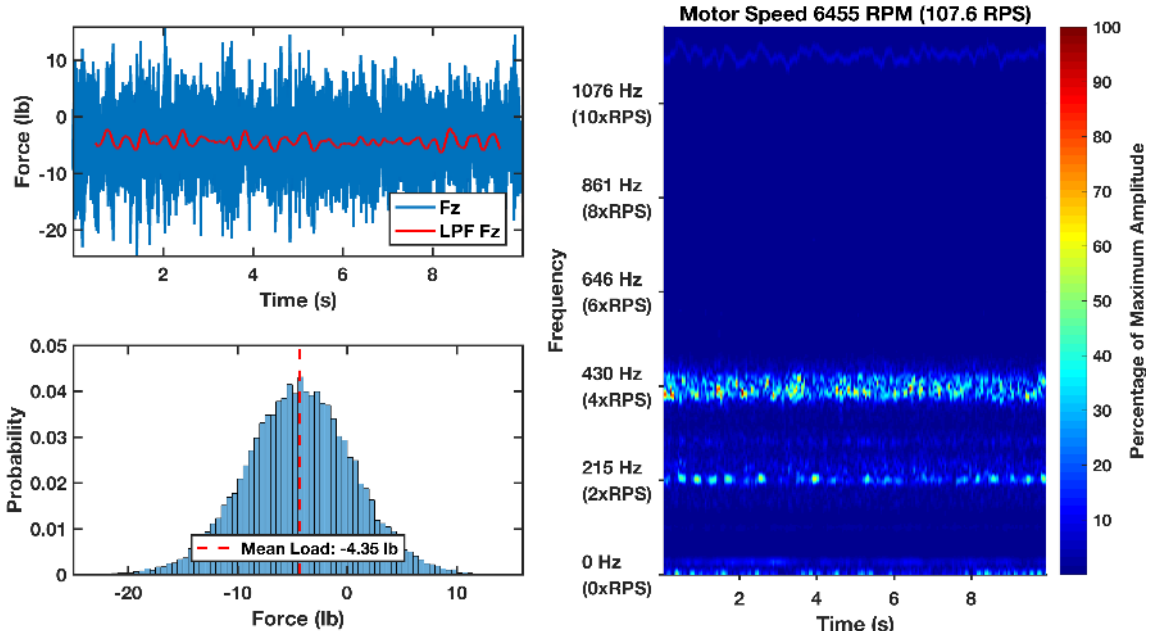


**Figure 7. Isolated rotor time-history and spectral analysis for force in z-direction (thrust). Incidence angle $i = -70°$, RPM = 6,455, V $= 37.8$ fps, J $= 0.30$. These are VRS conditions for the isolated rotor.**

forces observed, though the amount of amplification taking place due to the sting and balance assembly is presently unclear and a matter of ongoing investigation.

The time history data for each test condition were passed through a low-pass filter (LPF) in post processing for further analysis. The filter used is a second-order Butterworth filter with a -3 dB frequency of 6 Hz. The filter was applied using a zero-phase filtering process to eliminate phase distortion in the filtered data. In Fig. 6, no significant variation remains in the data after filtering; the filtered data are nearly constant and centered at the mean. For plotting and statistically analyzing the low-pass filtered data, the first and last 1/2 second of data were trimmed to eliminate filter transients occurring at theses edges.

Figure 7 provides an example of z-axis force (thrust) within the VRS region. Erratic modulation of the loading is seen in both the spectrogram and the force vs. time plots. The spectrogram reveals that the most significant frequency component corresponds to four cycles per rotation. Here, the LPF data displays very large variation about the mean. This characteristic is typical of rotor performance in VRS conditions[17].

### *4. Vortex Ring State Modeling*

Vortex ring state (VRS) is an operating condition wherein the rotor ingests its own tip-vortices and downwash in a sustained manner due to an up-flow of air (relative to the rotor disk) causing the wake of the rotor to be re-ingested from above. Fully-developed VRS might be visualized as a "donut" of air recirculating around the edges of the rotor disk.[7] VRS is an undesirable condition for a rotorcraft to operate in. It results in a significant loss of mean rotor thrust accompanied by unsteady low-frequency thrust variations; a reduction in responsiveness to inputs; and vibrations and uncommanded motion with an increased decent rate.[17] In helicopters, an uncorrected VRS condition often produces significant altitude loss, while in tiltrotor aircraft such as the V-22 VRS typically results in "roll-off" where the aircraft rolls to one side due to a thrust imbalance between its rotors. VRS encounter can present substantial difficulties with control particularly when the aircraft is close to the ground, such as might occur during the last stage of an approach to land.[7] In manned rotorcraft, pilots are trained to avoid VRS through careful control of decent rate and profile, and to monitor the aircraft carefully for symptoms of VRS when operating in conditions conducive to VRS development, such as steep approaches.[7] It is expected that VRS could pose a risk to autonomous sUAS rotorcraft where similar tasks of avoidance, detection, and recovery will fall to software and instrumentation on board the aircraft.

The approach taken here to modeling VRS for multirotor sUAS is based primarily on replicating two of its primary effects on rotor performance: reduction in mean rotor thrust, and unsteady thrust fluctuations. The conditions required for encounter of VRS have been shown to scale fairly well with non-dimensional velocity ratios of $V_x/v_h$ and $V_z/v_h$, where $V_x = V\cos i$, $V_z = V\sin i$, and $v_h$ is given by Eq. (1). This scaling term, $v_h$, is the momentum theory predicted induced velocity for a hovering rotor based on thrust, air density, and rotor disk area.[22,23]

$$v_h = \sqrt{T/(2\rho A)} \tag{1}$$

Examples of experimental VRS studies for various large-scale rotors can be found in Ref. [17] and the references therein. Various combinations of $V_x/v_h$ and $V_z/v_h$ in which full-scale rotorcraft are susceptible to VRS have been

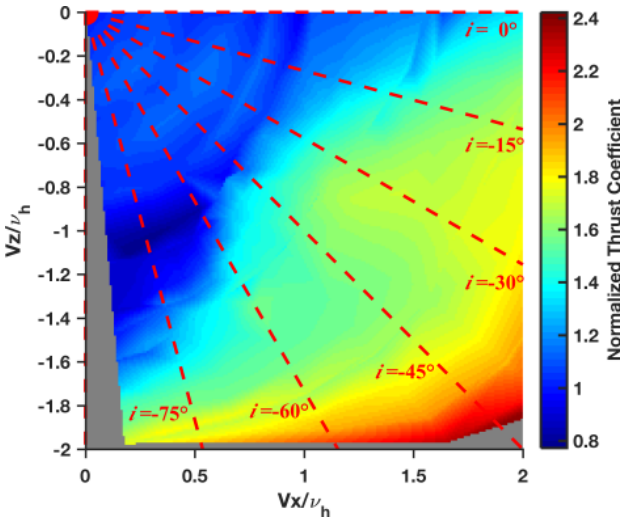


**Figure 8. Normalized thrust coefficient. VRS region appears in dark blue.**

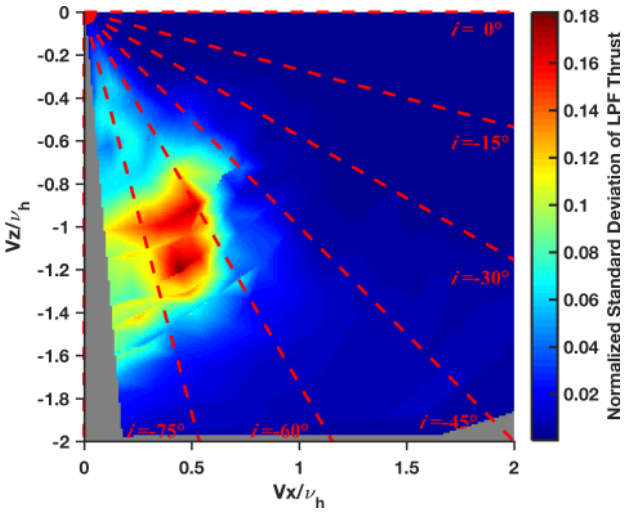


**Figure 9. Normalized standard deviation for low-pass filtered thrust. The VRS region shows intense low-frequency thrust variation.**

proposed, with relatively good agreement between the models. Isolated propeller testing conducted thus far during this research effort has produced results which appear comparable to these. Figure 8 shows variations in normalized thrust coefficient with $V_x/v_h$ and $V_z/v_h$. Here, normalized thrust coefficient is simply experimentally-measured thrust coefficient divided by the thrust coefficient obtained at hover conditions, where $C_{T,hover} = 0.011$.

Figure 9 shows the normalized standard deviation in low-pass filtered thrust, which provides a measure of the unsteadiness of thrust due to VRS. Here normalization is accomplished by dividing the standard deviation of the low-pass filtered time history data by the mean of the data. This allows comparison of thrust variation between runs where mean thrust differs substantially. However, this method is only reliable when the mean is significantly larger than zero, so runs at very low RPM are excluded. The specific frequency spectrum of the unsteady thrust variation has not yet been the subject of detailed analysis, though typical frequencies observed in these experiments appeared to be in the range of 1-3 Hz and appeared to vary with test conditions.

### E. Bare Airframe Test Results and Modeling

The bare airframe was tested at angles of attack ranging from -90 to +90 deg and at sideslip angles up to 45 deg. The tunnel speed was set at a dynamic pressure ($\bar{q}$) of 4 psf for all test points. The negative angles of attack were achieved by rolling the model inverted. The objective of these tests was to examine the fundamental aerodynamic stability characteristics of quadrotor vehicles and to develop a model suitable for implementation in a simulation for off-nominal conditions. While it is recognized that the airframe aerodynamic forces will typically be significantly less than propulsion forces, the importance of this model becomes apparent for forward flight conditions and during propulsion failure events. Selected test results are shown in Figs. 10-12.

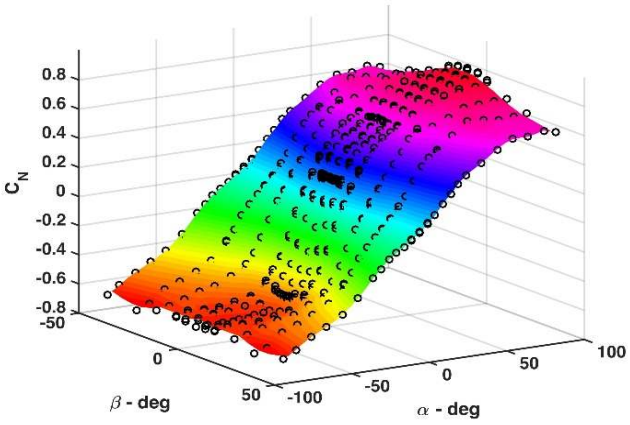


**Figure 10. Bare Airframe Aerodynamic Normal Force Coefficient.**

The normal force coefficient data shown in Fig. 10 indicates increasing force with increasing angle of attack although with lower magnitude than a similar size airfoil. The pitching moment coefficient shown in Fig. 11indicates unstable static pitch stability due to the increasing value of pitching moment with increasing angle of attack between approximately +/- 45 deg. Beyond these flow angles, the stability abruptly becomes positive as indicated by the change in slope. The rolling moment coefficient shown in Fig. 12 exhibits unstable static roll stability as shown by the positive rolling moment with increasing sideslip angles for all angles of attack.

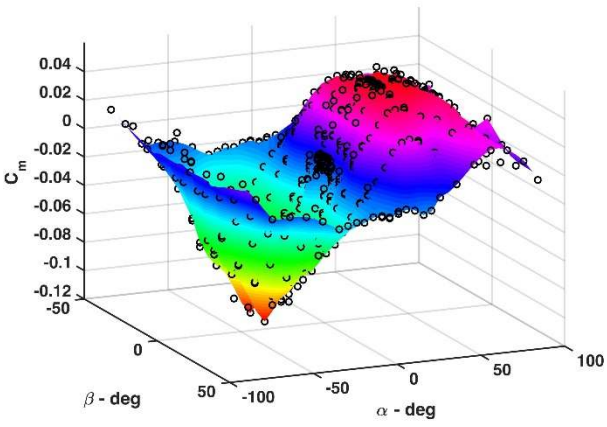


**Figure 11. Bare Airframe Aerodynamic Pitching Moment Coefficient.**

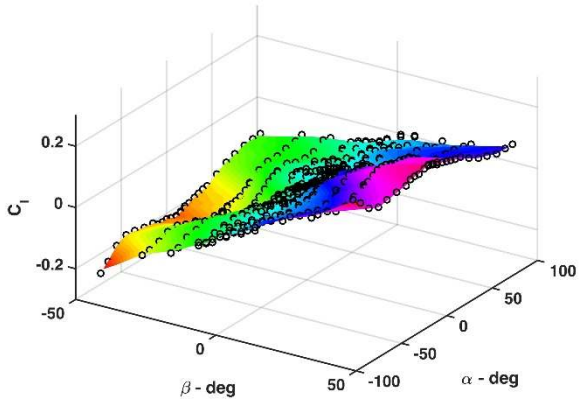


**Figure 12. Bare Airframe Aerodynamic Rolling Moment Coefficient.**

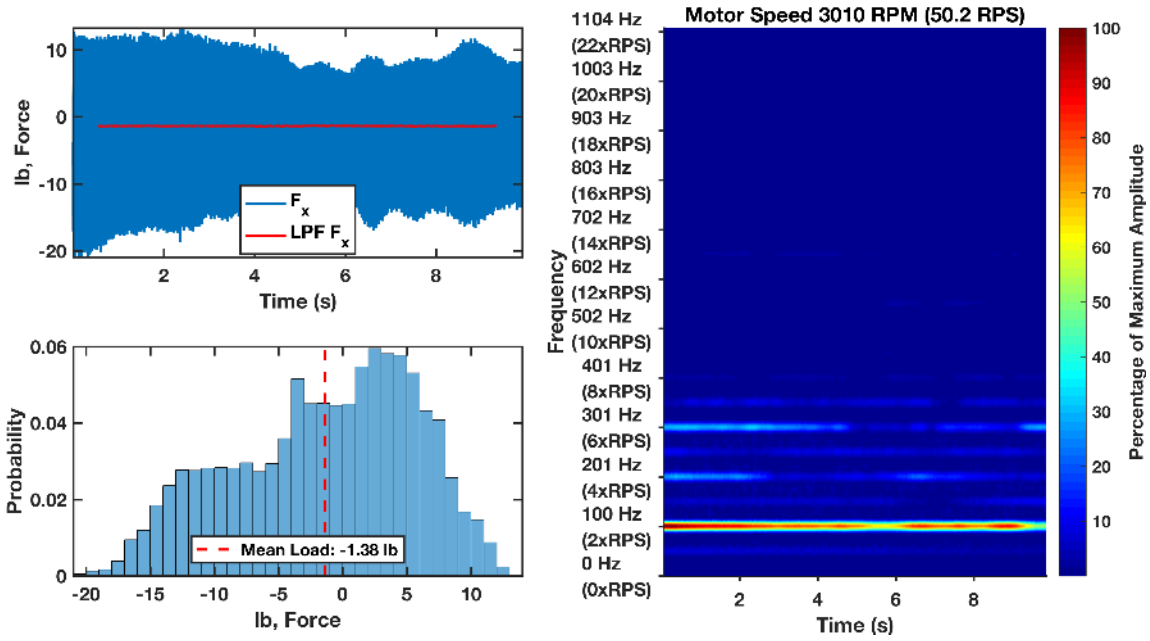


**Figure 13. Full-airframe time-history and spectral analysis for force in the x-direction. Aircraft angle of attack $\alpha = 0°$, RPM = 2,980 (all four rotors), V = 29 ft/s, J = 0.5.**

### F. Full-Airframe Testing

*1. Vibration characterization*

Substantial vibrations of intense magnitude were recorded during motors-on testing of the full airframe. These vibrations limited the availability to reach some desired test conditions because the balance's dynamic-load limits were approached. It was found that certain combinations of RPM, angle of attack, and tunnel speed produced excessive periodic loading, reaching balance dynamic-load limits in the body x-axis direction. This lead to most of the full-airframe testing being conducted at motor speeds of roughly 3,000 RPM or less to avoid reaching balance-load limits. Higher motor speeds were possible during the VRS-targeted runs, as the higher angle of attack (negative incidence angle) reduced the axial vibration to allowable levels. The full nature of these vibrations is somewhat unclear, but high-speed video has revealed that the arms of the aircraft underwent significant angular displacement at twice the frequency of the rotor, appearing to flex with each pass of the advancing blade. With the closed-loop RPM controller keeping all four rotors at nearly identical speeds, interactions between rotors due to their relative phase, and beat-frequency modulation of periodic loading due to small offsets in speed, are suspected to have played significant roles in the amplitude of the forces observed. The impact of vehicle flexing remains a topic for investigation and will be addressed in future testing.

An example of vibrations encountered for the full aircraft in edgewise relative wind ($\alpha = 0$ deg) is shown in Fig. 13. From the time-history and spectrogram, it appears that beating modulation may occur, with a long period exceeding the visible time-scale. The most significant frequency component is at twice the motor rotational speed (100.4 Hz), in contrast to the dominant frequency of four times the motor speed seen in isolated testing and appearing in Fig. 6. Note that despite the long period modulation, the mean force appears stable and that no movement is seen in the low-pass filtered data.

Figure 14 shows the full aircraft in VRS conditions. Here, $V_x/v_h = 0.51$ and $V_z/v_h = -0.88$, placing the aircraft very close to the conditions which produced maximum unsteadiness in isolated rotor thrust. There is a large and consistent frequency component at once-per motor rotation, and an intermittent component at twice-per motor rotation. The low-pass filtered data displays substantial low-frequency periodic thrust variations with a peak-to-peak amplitude of 3.26 lb, which represents a thrust fluctuation of about 15% of mean thrust. The average period of the fluctuation is about 0.74 seconds, or 1.35 Hz.

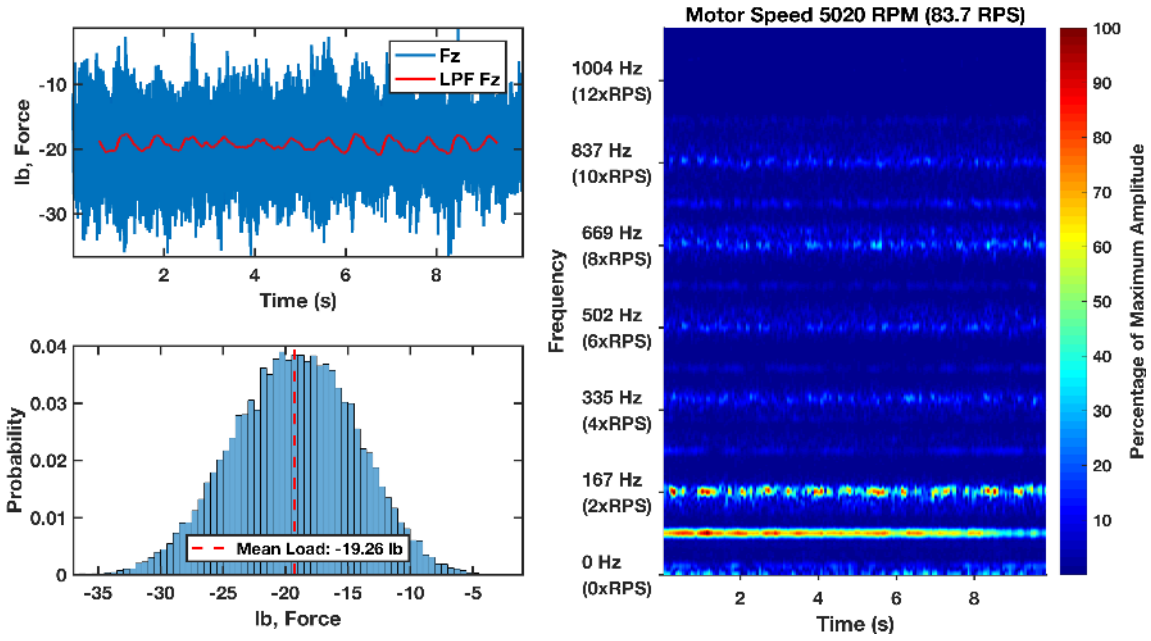


**Figure 14. Full airframe time-history and spectral analysis for force in z-direction. Aircraft-angle of attack $\alpha = 60°$, RPM = 5,020 (all four rotors), $V = 24\ ft/s$, $J = 0.25$. These are VRS conditions for the full-aircraft.**

VRS typically introduces uncommanded pitch or roll motion in multirotor sUAS, so unsteady moments are expected to be present. These moments could occur due to individual rotors experiencing differing degrees of VRS due to differences in operating conditions, or due to differences in the frequency or phase of the unsteady thrust variations affecting the individual rotors. Complex rotor-to-rotor wake interactions are also a possible sources of these moments. Figure 15 shows aircraft body-frame z-axis force ($F_z$) along with pitch ($M_y$) and roll ($M_x$) moments at the same test conditions as Fig. 14. It appears that there is a correlation between the variations in $F_z$ and $M_y$. The unsteady pitching moment generally follows, with some phase offset, changes in the thrust, and is larger than roll moment $M_x$. This indicates that for these conditions, the most likely un-commanded motion would be in the pitch direction, rather than roll. More extensive characterization of these behaviors is planned to improve the ability to model aircraft performance in VRS conditions.

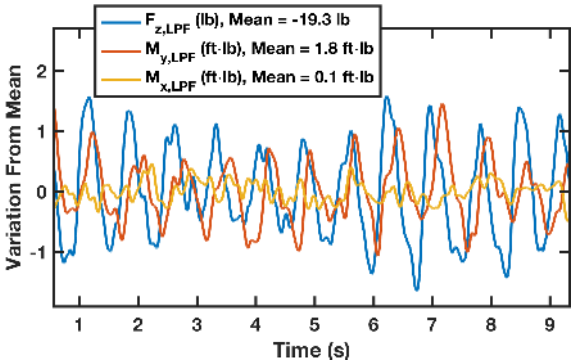


**Figure 15. Full-airframe time history of low-pass filtered data in VRS conditions. Aircraft angle of attack $\alpha = 60°$, RPM $= 5,020$ (all four rotors), $V = 24\ ft/s$, $J = 0.25$. Note apparent correlation of pitch moment ($M_y$) and thrust ($-F_z$)**

## V. Model and Simulation Development

### A. Software Architecture

A simulation was developed using the Mathworks MATLAB®/Simulink® environment to represent the dynamics of the aircraft in both nominal and off-nominal flight. The Simulink® model is parameter driven, with the representation of specific aircraft details such as total mass, motor placement, motor axis tilt, etc. imported at runtime from a MATLAB® data structure. This allows a single simulation model file to represent a broad range of multirotor aircraft and supports parametric variation studies. The simulation is organized into individual modules, with the most fundamental separation being the division of aircraft flight dynamics and control feedback. This structure makes is possible to isolate the influence of specific model features or selectively simplify the model to reduce computational cost and realism. It also allows straightforward modification to facilitate a broad range of other uses. Examples might

include control design, high-fidelity simulation of sensors and state-estimation performance, or realistic simulation of multi-agent systems of sUAS.

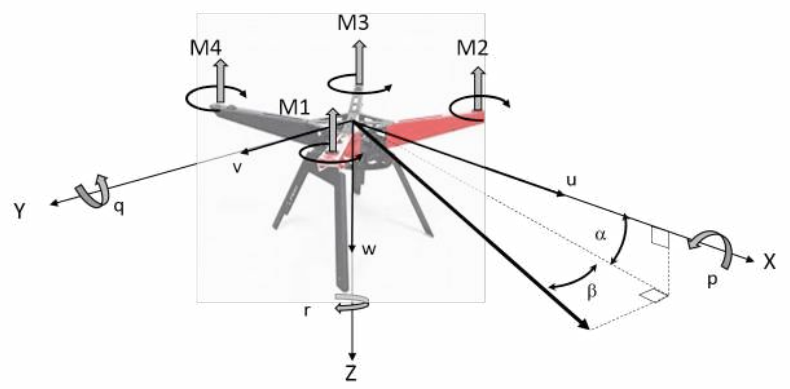


**Figure 16. Coordinates used for airframe performance model. Also shown are motor numbers and motor spin directions.**

### B. Equations of Motion

The flight dynamics model is based on six-degree-of-freedom rigid body dynamics. The equations of motion are defined within the body frame, as shown in Fig. 16, and the body frame forces ($\mathbf{F}^b$) and moments ($\mathbf{M}^b$) are appropriately specified to represent the various forces and moments acting on the quadrotor. A detailed explanation of the mathematical model is beyond the scope of this paper, but some of the fundamental features of the modeling approach are discussed here, particularly as they pertain to the incorporation of isolated rotor and airframe performance data.

In developing the model, the approach taken was to categorize forces and moments into propulsion, airframe, and interaction terms, based on their source. This organization is reflected by Eqs. (2) and (3).

$$\mathbf{F}^{\mathrm{b}} = \mathbf{F}^{\mathrm{b}}_{\mathrm{propulsion}} + \mathbf{F}^{\mathrm{b}}_{\mathrm{airframe}} + \mathbf{F}^{\mathrm{b}}_{\mathrm{interaction}} \quad \textbf{(2)}$$

$$\mathbf{M}^{\mathrm{b}} = \mathbf{M}^{\mathrm{b}}_{\mathrm{propulsion}} + \mathbf{M}^{\mathrm{b}}_{\mathrm{airframe}} + \mathbf{M}^{\mathrm{b}}_{\mathrm{interaction}} \quad \textbf{(3)}$$

This structure serves several purposes in the model development. First, it describes the methodology for wind tunnel testing of the aircraft, which has involved isolated-motor testing, isolated-airframe testing, and full-aircraft testing. The influence of the interaction term can be identified by taking wind tunnel measured full-aircraft data (taken as $\mathbf{F}^b$ and $\mathbf{M}^b$) in combination with the forces and moments measured during isolated-rotor testing. This approach allows a more structured view of how individual aspects of the vehicle's aerodynamic characteristics influence flight performance under different operating conditions. This method of organization may also provide insight into what areas of the vehicle's dynamic envelope are likely to be challenging for autonomous aircraft, since conditions where large-magnitude interaction terms appear may be more likely to pose controller performance issues or be indicative of complex underlying aerodynamics.

Each of the terms in Eqs. (2) and (3) are represented individually in the simulation as a subsystem. Lookup tables for performance coefficients as a function of flight condition are loaded from the MATLAB® workspace. The lookup tables can be generated using linear interpolation directly on wind tunnel data, or polynomial fits of the data. Both approaches are currently used depending on the behavior of the dataset, and future testing is planned to further refine these tables. The independent parameters on which the performance coefficients depend vary for each term: the propulsion terms currently utilize primarily dimensionless rotor velocity ratios $\mu_x$ and $\mu_z$ for coefficient lookup, while the isolated-airframe performance coefficients are a function of angle of attack ($\alpha$) and sideslip ($\beta$), defined as in Fig. 16. Characterization of the interaction term is currently in progress and remains the subject of ongoing research.

### C. Propulsion Model

Throughout the flight-envelope, multirotor sUAS vehicles dynamics are largely dominated by forces and moments from the rotor system. Rotor performance varies significantly with operating condition. This performance dependence can be described in terms of non-dimensional parameters. For the purposes of modeling off-nominal performance, the data collected from isolated propeller testing suggests a reasonable choice of primary independent parameters for are the rotor advance ratio ($\mu_x$) and normal velocity ratio ($\mu_z$), given in Eqs. (4) and (5).

$$\mu_x = \frac{\mathrm{V}}{\Omega \mathrm{R}}\cos(i), \quad \mu_z = \frac{\mathrm{V}}{\Omega \mathrm{R}}\sin(i) \quad \textbf{(4), (5)}$$

These and other rotor dimensionless parameters are described in Refs. [22], and [23]. A diagram related to these terms is shown in Fig. 3. Other influences on performance are also expected[19], though. Influences such as Reynolds number can be seen in the test results and have been discussed in the literature.

An alternative (but essentially equivalent) parameter choice is to use propeller advance ratio ($J = V/(RPS \cdot D)$) and incidence angle ($i$). Conversion between ($\mu_x$, $\mu_z$) and (J, $i$) coordinates is direct and straightforward: $J = \pi\sqrt{\mu_x^2 + \mu_z^2}$ and $i = \text{atan}(\mu_z/\mu_x)$. In building lookup tables for simulation in terms of incidence angle and velocity ratio, use of $\mu_x$ and $\mu_z$ coordinates appears to be preferable since as airspeed (V) approaches zero (i.e. hover conditions), both parameters also converge toward zero, which is not the case for $i$.

Rotor performance can be represented in terms of dimensionless coefficients. The most fundamental to multirotor flight modeling are the thrust ($C_T$) and torque ($C_Q$) coefficients, given by Eqs. (6) and (7), though other important coefficients such as those for pitch and roll-moment are also important influences on multirotor performance in forward flight. Wind tunnel testing has shown that significant variation in these parameters occurs with changing flight conditions, and especially with variation of $\mu_x$ and $\mu_z$.

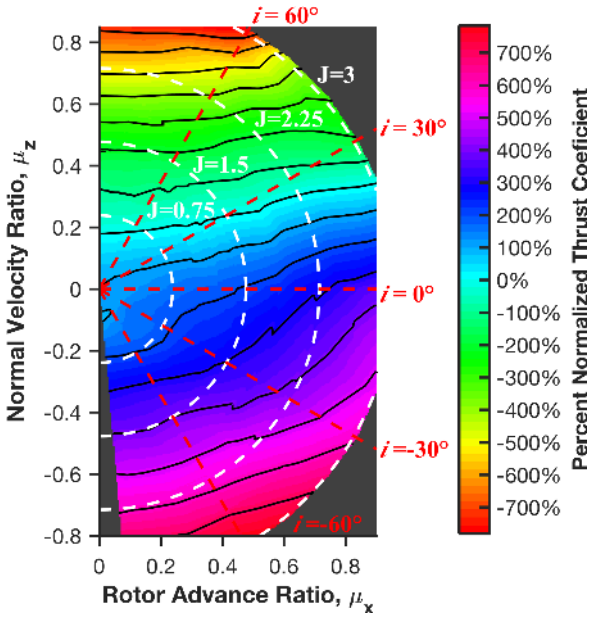


**Figure 17. Isolated rotor normalized thrust coefficient.**

Figure 17 shows percent normalized thrust coefficient for a wide range of the conditions tested for the isolated rotor. The normalized thrust coefficient is defined here as the thrust coefficient observed for a given test condition

$$C_T(\mu_x, \mu_z) = \frac{T(\mu_x, \mu_z)}{\rho A(\Omega R)^2}, \qquad C_Q(\mu_x \mu_z) = \frac{Q(\mu_x, \mu_z)}{\rho A(\Omega R)^2 R} \tag{6), (7}$$

divided by the thrust coefficient value found at hover conditions ($\mu_x = \mu_z = 0$). Assuming an aircraft weight of 6.16 lb and $C_{T,hover} = 1.10\times10^{-2}$ from the isolated rotor data, the required motor speed in hover is approximately 3,840 RPM. From the scale of the variation in the thrust coefficient shown, it is clear that a simulation model developed assuming constant $C_T$ could dramatically under- or over-predict thrust production especially in conditions where $\mu_z$ is large in magnitude.

Figure 18 shows a detail view of the same data. The area of depression in $C_T$ appears as the isolated yellow area at incidence angles below 60° and a propeller advance ratio of 0.25. To put the location of this feature in perspective: at a hover motor speed of 3,840 RPM, this region would be encountered at descent velocities of around 18 ft/s. This area is associated with the development of VRS. It should be noted however that a better predictor of VRS, especially across different aircraft at different scales, is the region shown in Figs. 8 and 9, which scales with thrust (via Eq. (1)) rather that rotor speed, which is a meaningful distinction.

For simulation purposes, wind axes are calculated for each motor, and $\mu_x$ and $\mu_z$ are formed. For each rotor, performance coefficients are found from a lookup table based on $\mu_x$ and $\mu_z$. The performance coefficients are then used to compute motor wind axes force and moment vectors, and then to compute aircraft body frame forces and moments based on motor placement relative to the aircraft center of mass.

Motor dynamics are assumed to be given by a model similar to what is proposed in Ref. [24], which includes a first-order differential equation with low-pass filter dynamics. The model presently used cannot account for

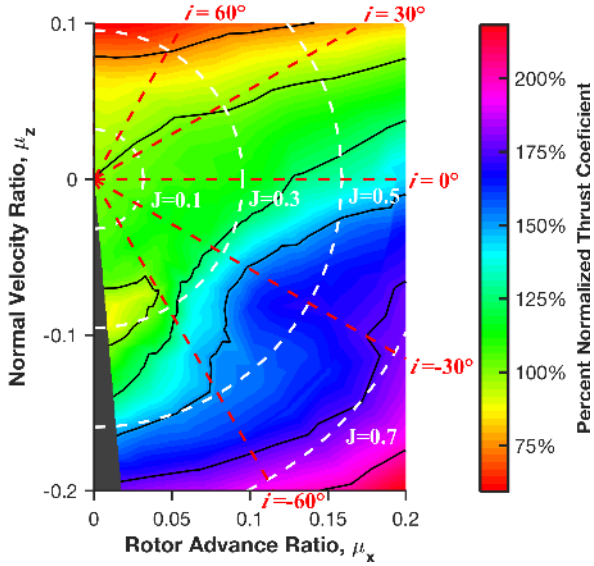


**Figure 18. Detail near VRS region: isolated rotor normalized thrust coefficient.**

windmilling behavior correctly, and may over-predict available torque during powered flight as it implicitly assumes that adequate power is available to keep the time-constant of the motor dynamics constant. Improving the fidelity of the motor model, particularly with respect to wind milling and torque limitations, is planned as future work.

### D. Aerodynamic Model Integration

The aerodynamic model from isolated airframe testing is incorporated to account for the influence of the aircraft body on performance. Lookup tables are used which return force and moment coefficients as a function of body wind axes coordinates. It should be noted that in general these are not identical to the motor-wind coordinates. These forces and moments are summed with the propulsion model forces and moments in accordance with Eqs. (2) and (3). Interactions between the rotors, and between the rotors and the airframe, are not accounted for by these calculations. Instead, these will be accommodated by the interaction term. While the influence of the isolated-airframe forces and moments during slow flight is small relative to that of the rotors, at high speeds and especially during motor failures, the isolated airframe forces are expected to play an important role in determining the trajectory of the aircraft.

### E. Avionics Emulation

Multirotor sUAS performance is heavily dependent on the actions of the control system, especially in off-nominal conditions. Any effort to predict aircraft trajectory must take into account the behavior of the controller if the motors are still powered. The present form of the simulation utilizes a control structure fairly typical for sUAS multirotors; there is an inner-loop which regulates attitude, while an outer loop (or loops) provide attitude commands to control position or track sequenced waypoints. No sensor models are yet included in the simulation, so state feedback is used for control. As the current focus is on flight-dynamics simulation development, the simulation does not yet include a rigorous simulation of a specific sUAS avionics and control system, though the structure of the simulation could accommodate such extensions.

For the preliminary simulation results demonstrated here, only an inner-loop attitude and altitude controller will be needed. A state feedback controller designed using a linearized model of the aircraft about an equilibrium hover condition is used for this purpose. The controller gains are optimized using the robust servomechanism Linear Quadratic Regulator (LQR) design process.[25] This controller regulates twelve aircraft states; these include angular velocity, attitude, altitude, and the 4 motor speeds. In addition, the controller internally regulates integral error in attitude and altitude. The integral action of the controller is needed to maintain stability and robust reference tracking in light of the significant parameter variations introduced in the model. Because state feedback is available in the simulation, and because the linearized model is accurately known, this controller can be tuned to perform more aggressively then would likely be possible for real-world aircraft subject to sensor limitations and model inaccuracies. Thus, to increase realism the simulation controller is intentionally detuned slightly, to make performance more representative of real aircraft.

### F. Modeling VRS Effects on Performance

A prototype method to simulate the VRS behavior of the aircraft has also been included. This simulation method is based on replicating the presence of unsteady low-frequency thrust fluctuations, with the reduction in mean thrust accomplished via table lookup of $C_T(\mu_x, \mu_z)$. This approach does not account for VRS induced velocity directly, as in Ref [17]. Instead a time-varying thrust coefficient variation is introduced, based in part on experimental data, in an attempt to replicate the effects of VRS. The model used for variation of thrust coefficient during VRS conditions is given in Eq. (8).

$$C_{T_{VRS}} = C_T(\mu_x, \mu_z)\left(1 + \mathrm{A_{VRS}}\ \cos\left(\omega_{\mathrm{VRS}} t + \delta(t)\right)\right) \tag{8}$$

This term is computed separately for each of the motors. The amplitude term $\mathrm{A_{VRS}}$ is based on a lookup table representation of the data shown in Fig. 9. The frequency $\omega_{\mathrm{VRS}}$ is a constant chosen to roughly match the thrust variation frequencies seen in the test data, and $\delta(t)$ is a time-varying random-walk phase offset, tuned to provide variations in the relative phase of the $C_{T_{VRS}}$ for each of the motors. While this model has obvious limitations, and is not based on the changes to induced velocity that more accurately drive real VRS performance, it appears to produce behavior generally matching expectations for VRS encounter. Improvements to VRS modeling and simulation are an area for future work.

## VI. Preliminary Simulation Results

Ongoing research under the UTM program is addressing important off-nominal scenarios based on proposed use cases and anticipated failure states.[1–4] It is intended to use the simulation to study failure scenarios and to support development of risk assessment tools. The simulation has been designed to model aircraft performance beyond the

nominal flight envelope and situations such as individual or complete motor failure can easily be introduced in the simulation. However, windmilling effects are not yet well modeled, and therefore motor failure is considered only representative of a stopped rotor. It is likely that in some cases, windmilling would occur, generating substantial forces and moments and changing the characteristics of the aircraft's free-fall trajectory. Other types of motor failure, such as stuck throttle or partial power failures, are likely more reliably replicated by the present model.

Three representative scenarios were selected to assess the feasibility of the modeling approach and to provide preliminary qualitative data for risk analysis.

Case 1: Abrupt failure of all four motors during forward flight (rotors fully stopped)
Case 2: Stuck throttle on all four motors during forward flight
Case 3: VRS encounter during descent (no failure)

It should be noted that following the failure, Cases 1 and 2 are not appreciably influenced by controller design, while performance in Case 3 is affected by controller performance. In all three examples, the controller used is the state feedback attitude and altitude tracking control; position control and waypoint sequencing modes are disengaged.

*1. Abrupt failure of all four motors during forward flight*

Time histories for a complete failure of all four motors during forward flight are shown in Fig. 19. The aircraft begins from a stationary hover at 400 ft, and immediately begins tracking an attitude command which ramps up to a pitch of -20 deg. The aircraft has nearly reached equilibrium conditions on a north heading when the failure occurs at 15 seconds. This failure leads to a rapid departure from a nominal flight attitude as indicated by the rapid onset of nose-down pitch rate/tumbling accompanied by highly dynamic pitch oscillations. No significant roll or yaw motions appear until about 5 seconds after failure. Following failure, the vehicle essentially follows a ballistic trajectory leading to ground impact after approximately 6 sec. The trajectory remains primarily along the direction of flight, with no notable sideward motion before impact.

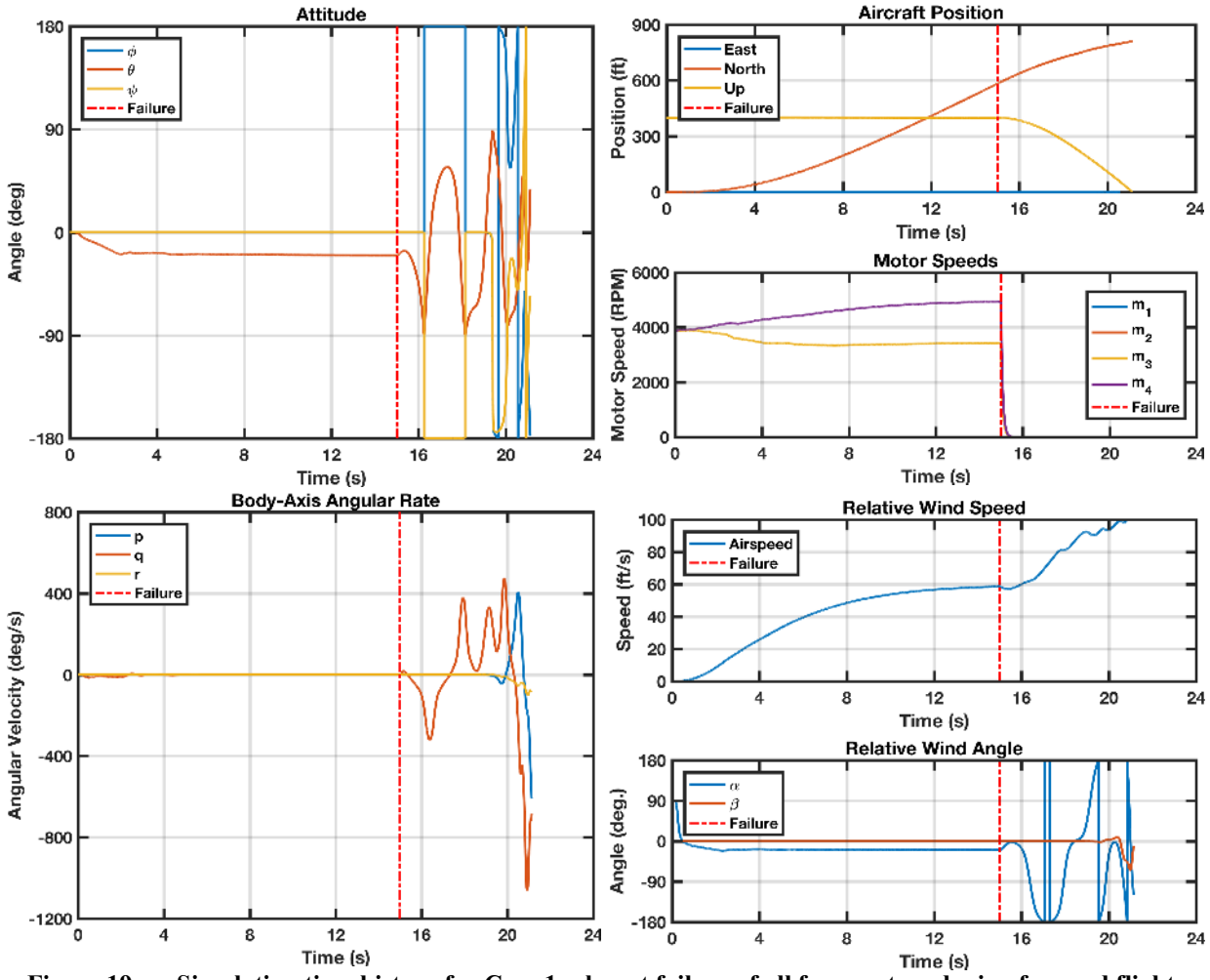


**Figure 19. Simulation time history for Case 1: abrupt failure of all four motors during forward flight.**

*2. Stuck throttle on all four motors during forward flight*

Figs. 20 and 21 show simulation results for stuck throttle of all four motors during forward cruise flight. Preceding the stuck throttle failure, conditions are identical to Case 1. Immediately following the failure, the aircraft undergoes a slight nose up, generating a small increase in altitude. The flight condition rapidly deteriorates from about 17 sec on, with the aircraft beginning to tumble at high angular rates. This tumble exhibits negative pitching rotation, but quickly transitions to more complex rotation. This motion generates significant kinematic coupling as indicated by the large values of α and thus different aerodynamic loading on each of the motors, which depart from their original speeds as a result. As no testing has been performed to assess the influence of rates on aerodynamic coefficients, these results suggest a need for improved model fidelity during high rate conditions to better describe performance during such extreme off-nominal conditions. Also notable is the predicted airspeed, which during the crash trajectory is less than what is predicted for the complete motor failure shown in Fig. 19. The impact trajectory veers to the right of the original flight path by 48 ft.

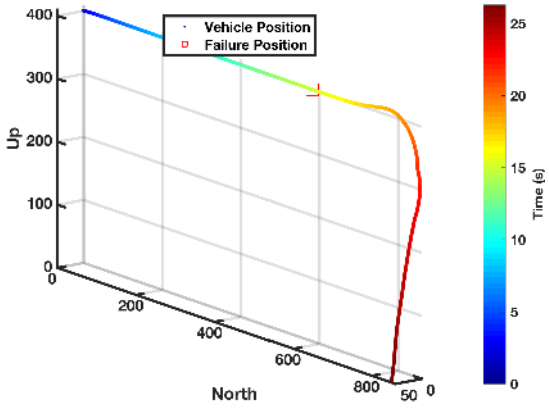


**Figure 20. Case 2 trajectory**

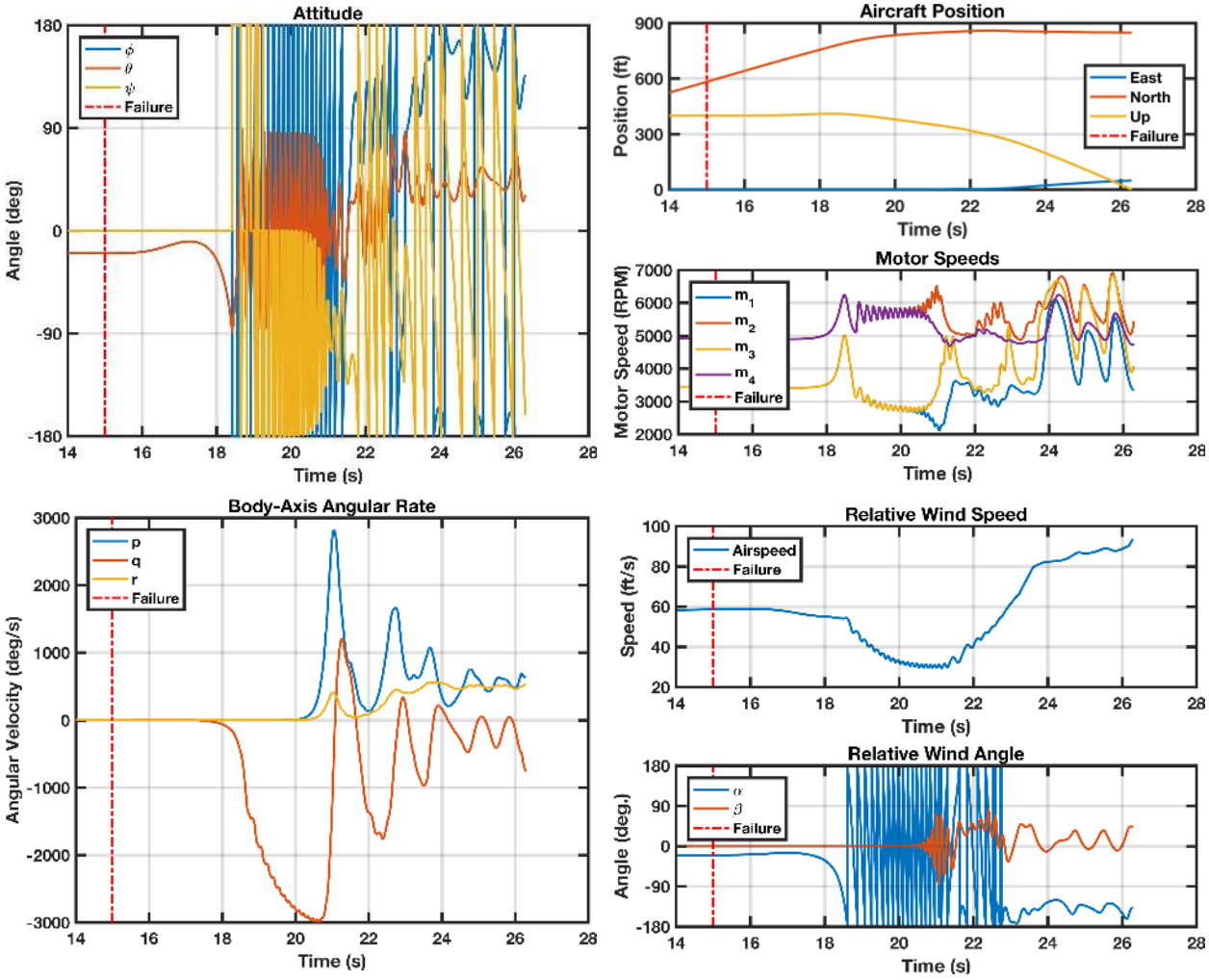


**Figure 21. Simulation time history for Case 2: stuck throttle on all motors during flight**

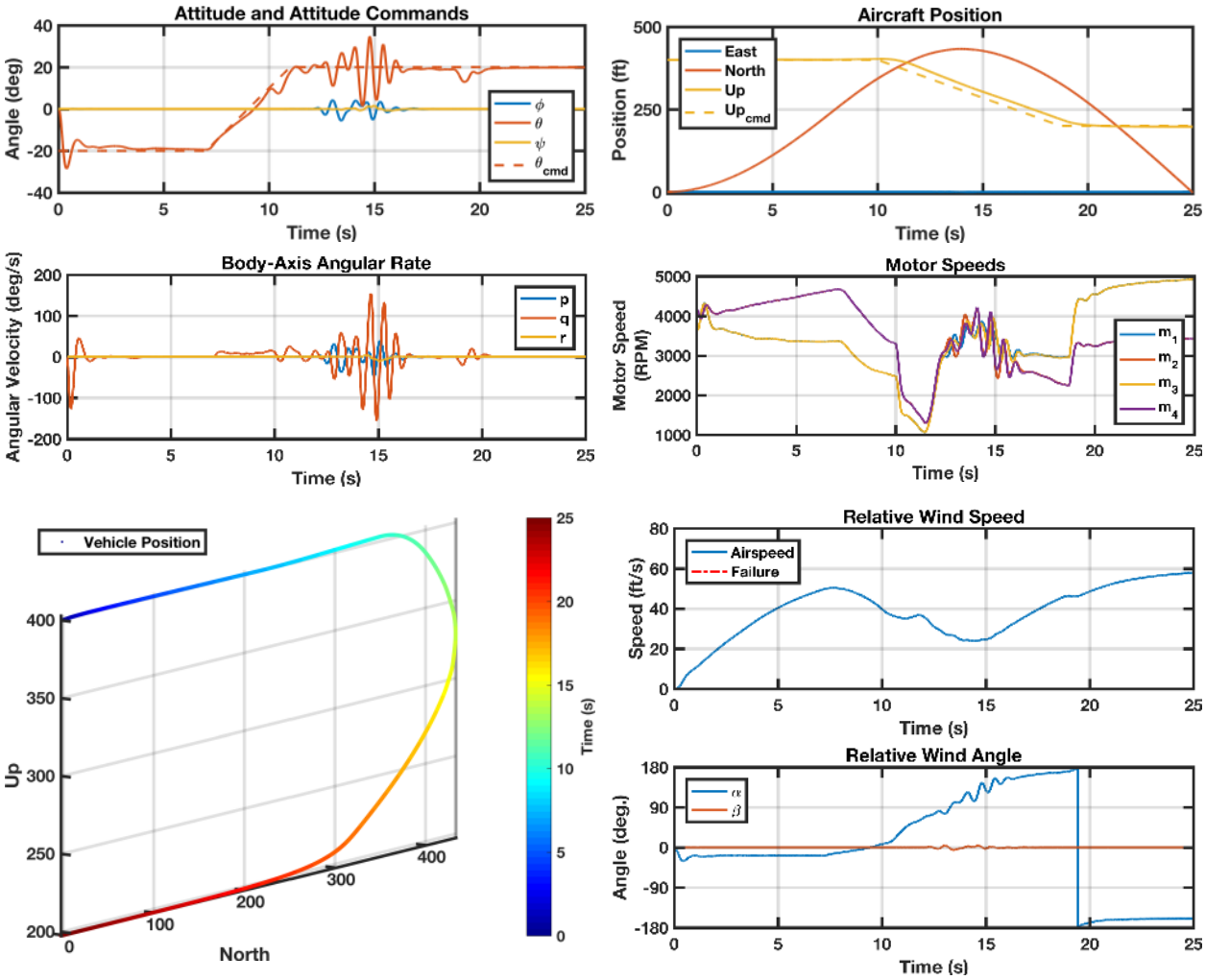


**Figure 22. Simulation time history for Case 3: VRS encounter during descent.**

*3. VRS encounter during decent*

A maneuver resulting in VRS encounter is shown in Fig. 22. The aircraft begins in a hover and rapidly transitions to forward flight by pitching forward 20 deg. The pitch direction is reversed beginning at 7 seconds, resulting in a decrease in forward speed. A descent is initiated from 400 ft to 200 ft beginning at 10 seconds. The combination of airspeed and decent angle results in $V_x/v_h$ and $V_z/v_h$ values associated with VRS as shown in Fig. 23. The observed behavior is generally in agreement with expectations for multirotors experiencing VRS. Significant pitch oscillations, and less intense roll motions are seen to result from the VRS thrust modulation. The difference in pitch and roll motion is largely attributable to the relative phase of the modulation amplitude signals; different phase offsets produce differing oscillations in pitch or roll as a result of the random phase variable in Eq. (8). It is notable that the altitude of the vehicle is not appreciably affected, and that the mean attitude appears to track the desired value. This is largely due to the aggressive actions of the controller,

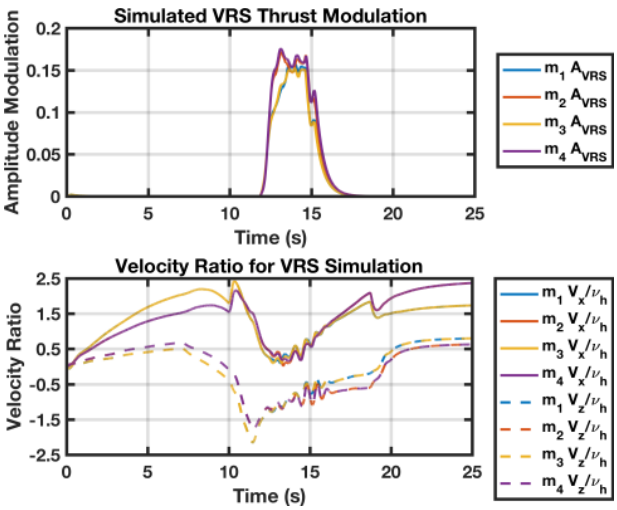


**Figure 23. Simulation time history of VRS-related parameters for Case 3.**

made possible by full-state feedback. A controller without full state feedback and subject to sensor limitations would likely have more difficulty maintaining control of attitude and altitude.

## VII. Summary and Future Plans

A preliminary high-fidelity simulation of a quadrotor sUAS vehicle has been developed to support risk assessment and safety analysis for the NASA UTM program. A series of wind tunnel tests of a COTS quadrotor were completed which included force and moment measurements for an isolated propulsion system, the bare airframe, and a complete powered airframe. A unique aerodynamic and propulsion database for large wind incidence angles, representative of extreme off-nominal events, was developed from the wind tunnel data. Primary objectives of this research were to define model requirements and to explore wind tunnel test methods specific to multi-rotor vehicles in off-nominal conditions.

Based on the isolated propulsion testing, the effects of flow angle, relative to the rotor, were clearly demonstrated and showed that this effect must be modeled for reliable prediction of off-nominal events. In addition, vortex ring state behaviors were identified and were found to be consistent with previous test results for full-scale rotorcraft and isolated sUAS propellers. An empirical modeling approach that introduces the time-varying thrust fluctuations present during VRS has been proposed and demonstrated to provide a reasonable representation of multirotor behavior during VRS encounter. Vibration effects were found to be significant and consistent with previous published results. These vibrations introduced large dynamic balance loads which limited the selection of wind tunnel conditions tested. Vibration effects were determined to be partially due to inertial loads unique to the model installation and research is ongoing to explore methods to mitigate these effects as well as to develop methods for improved data reduction.

The bare airframe testing yielded consistent results which showed clear trends in aerodynamic static stability which are important for trajectory prediction. Notably, although the test vehicle has no airfoil lifting surfaces, the force and moment trends were consistent with typical fixed-wing vehicles in terms of modeling approach and interpretation of data. The importance of modeling the airframe aerodynamics was shown for certain failure conditions. Furthermore, these results highlighted the need for accurate aerodynamic models of multi-rotor airframes that are enclosed or have significant aerodynamic shaping for optimized cruise performance.

The powered airframe test provided data that will be used to identify aerodynamic effects due to the interaction between the airframe and propulsion system. However, vibration effects were significant, as seen during isolated propulsion testing, which excluded testing of some conditions. Vehicle flexing under the imposed loads was found to have some influence on the vibration characteristics and this remains a topic for further study.

A preliminary six degree-of-freedom simulation was developed using the Mathworks MATLAB®/Simulink® environment that incorporated the propulsion and airframe database from the wind tunnel testing. Several simulation test scenarios related to motor failure or rapid descent were selected to demonstrate the effects of non-linear aerodynamic and propulsion modeling features necessary for predicting performance for out-of-envelope conditions. The complex nature of multirotor dynamics, such as the high angular rates and erratic trajectories shown from the simulation results, demonstrated the modeling challenges associated with predicting off- nominal trajectories for these vehicles. Development of the simulation will continue with the objective of validating the potential of a generic representation for n-rotor vehicles and to support development of low-order modeling and prediction methods.

This research highlighted the need for test and modeling methods specific to sUAS multi-rotor vehicles in off-nominal conditions, primarily due to the complex aerodynamic characteristics of rotors that are inclined to the relative wind. Future isolated rotor testing will include a more complete set of RPM measurements that are time correlated with the strain gauge balance measurements. In addition, the effect of angular rate of the rotor system relative to the freestream will be the subject of future testing. It is anticipated that flow visualization and high-speed video will be used to further study vibration effects as well as vortex ring state flow behaviors.

## Acknowledgments

The authors would like to acknowledge Ms. Sue Grafton, Mr. Mario Smith, and Mr. Ron Busan for significant contributions to the wind tunnel testing.

Author David Hartman's contributions to this material were supported in part by funding from the National Science Foundation Graduate Research Fellowship Program under Grant No. DGE-1646737. Any opinions, findings, and conclusions or recommendations expressed in this material are those of the authors and do not necessarily reflect the views of the National Science Foundation.

## References


[1] Barr, L. C., Newman, R. L., Ancel, E., Evans, J. K., Foster, J. V., Belcastro, C. M., and Klyde, D. H., "Preliminary Risk Assessment for Small Unmanned Aircraft Systems," *AIAA Aviation Forum (submitted for publication)*, 2017.

[2] Belcastro, C. M., Newman, R. L., Evans, J. K., Klyde, D. H., Barr, L. C., and Ancel, E., "Current and Future Hazards Identification and Analysis for Unmanned Aircraft System (UAS) Operations," *AIAA Aviation Forum (submitted for publication)*, 2017.

[3] Ancel, E., Foster, J. V., and Condotta, R., "Real-time Risk Assessment Framework for Unmanned Aircraft System (UAS) Traffic Management (UTM)," *AIAA Aviation Forum (submitted for publication)*, 2017.

[4] Belcastro, C. M., Klyde, D. H., Logan, M. J., Newman, R. L., and Foster, J. V., "Experimental Flight Testing for Assessing the Safety of Safety-Critical Unmanned Aircraft System Operations," *AIAA Aviation Forum (submitted for publication)*, 2017.

[5] Chambers, J. R., "High-Angle-of-Attack Technology: Progress and Challenges in High-Angle-of-Attack Technology," *NASA CP-3149*, 1992.

[6] Foster, J., Cunningham, K., Fremaux, C., Shah, G., Stewart, E., Rivers, R., Wilborn, J., and Gato, W., "Dynamics Modeling and Simulation of Large Transport Airplanes in Upset Conditions," *AIAA Guidance, Navigation, and Control Conference and Exhibit*, 2005, p. 5933.

[7] U.S. Department of Transportation, Federal Aviation Administration, Flight Standards Service, *Helicopter Flying Handbook*, FAA-H-8083-21A, .

[8] Mahony, R., Kumar, V., and Corke, P., "Multirotor Aerial Vehicles," *IEEE Robotics and Automation Magazine*, vol. 20, 2012.

[9] Martin, P., and Salaün, E., "The True Role of Accelerometer Feedback in Quadrotor Control," *IEEE International Conference on Robotics and Automation (ICRA)*, IEEE, 2010, pp. 1623–1629.

[10] Mueller, M. W., and D'Andrea, R., "Relaxed Hover Solutions for Multicopters: Application to Algorithmic Redundancy and Novel Vehicles," *The International Journal of Robotics Research*, vol. 35, 2016, pp. 873–889.

[11] Efraim, H., Shapiro, A., and Weiss, G., "Quadrotor with a Dihedral Angle: On the Effects of Tilting the Rotors Inwards," *Journal of Intelligent & Robotic Systems*, vol. 80, 2015, p. 313.

[12] Mellinger, D., Michael, N., and Kumar, V., "Trajectory Generation and Control for Precise Aggressive Maneuvers with Quadrotors," *The International Journal of Robotics Research*, vol. 31, 2012, pp. 664–674.

[13] Hehn, M., and D'Andrea, R., "Real-Time Trajectory Generation for Quadrocopters," *IEEE Transactions on Robotics*, vol. 31, 2015, pp. 877–892.

[14] Hoffmann, G., Huang, H., Waslander, S., and Tomlin, C., "Quadrotor Helicopter Flight Dynamics and Control: Theory and Experiment," *AIAA Guidance, Navigation and Control Conference and Exhibit*, 2007, p. 6461.

[15] Betzina, M. D., "Tiltrotor Descent Aerodynamics- A Small-Scale Experimental Investigation of Vortex Ring State," *AHS International Annual Forum, 57th, Washington, DC*, 2001.

[16] Abrego, A. I., Betzina, M. D., and Long, K. R., *A Small-Scale Tiltrotor Model Operating in Descending Flight*, NASA Moffett Field, CA, Rotorcraft Division, 2002.

[17] Johnson, W., *Model for Vortex Ring State Influence on Rotorcraft Flight Dynamics*, NASA/TP-2005-213477, 2005.

[18] Theys, B., Dimitriadis, G., Andrianne, T., Hendrick, P., and De Schutter, J., "Wind Tunnel Testing of a VTOL MAV Propeller in Tilted Operating Mode," *International Conference onUnmanned Aircraft Systems (ICUAS)*, IEEE, 2014, pp. 1064–1072.

[19] Brandt, J., and Selig, M., "Propeller Performance Data at Low Reynolds Numbers," *49th AIAA Aerospace Sciences Meeting*, Orlando, FL: 2011.

[20] Shetty, O., and Selig, M., "Small-Scale Propellers Operating in the Vortex Ring State," *49th AIAA Aerospace Sciences Meeting*, Orlando, FL: AIAA, 2011.

[21] Russell, C. R., Jung, J., Willink, G., and Glasner, B., "Wind Tunnel and Hover Performance Test Results for Multicopter UAS Vehicles," *merican Helocipter Society 72nd Annual Forum*, West Palm Beach, FL: 2016.

[22] Leishman, G. J., *Principles of Helicopter Aerodynamics*, Cambridge university press, 2006.

[23] Johnson, W., *Rotorcraft Aeromechanics*, Cambridge University Press, 2013.

[24] Stevens, B. L., Lewis, F. L., and Johnson, E. N., *Aircraft Control and Simulation: Dynamics, Controls Design, and Autonomous Systems*, Hoboken, New Jersey: John Wiley & Sons, 2016.

[25] Lavretsky, E., and Wise, K. A., *Robust Adaptive Control with Aerospace Applications*, Springer, 2013.